



Concentration fluctuations modeling: a comparative study

Alon Manor¹

Received: 1 May 2022 / Accepted: 10 October 2022 / Published online: 27 October 2022
© The Author(s), under exclusive licence to Springer Nature B.V. 2022

Abstract

Two recently reported models, the Virtual Variance Sources (VVS) model and the Volumetric Particle Approach (VPA), both predicting the second moment of passive scalar concentration fluctuations in the atmosphere caused by a localized source of gas, are comparatively studied. Both models operate within the framework of a Lagrangian Stochastic Particle Model. Meteorological and tracer data from project Sagebrush phase 1 experiment are used to examine the models for real meteorological data for a localized ground source scenario under the same conditions and parametrizations, including dissipation timescale parametrization. As a reference, the simple scaling model of Chatwin and Sullivan (CS) was also applied. Both the VVS model and the VPA reasonably predict the concentration variance. Notably, the CS model yields comparable results to its more sophisticated counterparts. In addition to comparison to statistics of high frequency concentration measurements, important applicative aspects of the models were studied. The VPA is found to exhibit better statistical convergence demanding less particles, and relatively low sensitivity to dissipation timescale.

Keywords Concentration fluctuations · Stochastic Lagrangian particle model · Project Sagebrush

1 Introduction

Concentration up to a few kilometers downwind from a localized continuous source emitting gas into the atmospheric boundary layer exhibits considerable intermittency. This implies that instantaneous concentration can reach values a few times higher than the time averaged concentration measured at the same location [1, 2]. Taking this phenomenon into consideration can be important for many applications for which short period or instantaneous concentration is of interest. These include hazard assessment for flammable or highly toxic agents [3], estimation of odor nuisance [4] and dynamic source tracking [5].

The Lagrangian Stochastic Particle modeling framework is based on the notion that the turbulent transport of marked air parcels can be modelled using Langevin stochastic equations, in analogy with Brownian motion of thermal molecules [6]. This approach has been

✉ Alon Manor
alonmanor@gmail.com

¹ Israeli Institute for Biological Research, Ness Ziona, Israel

recognized as a mature method for atmospheric transport and diffusion (T&D) calculations. It can successfully handle complex topography, urban or natural canopy, ground or elevated sources. However, within an LSPM, the dynamics of every particle, simulating an air parcel transported by the turbulent flow, is considered separately from the other particles. Every single trajectory is a possible realization, and the ensemble average over many trajectories can be interpreted as the average of a long enough time period for which turbulence is stationary. Thus, by design, the LSPM can give estimations regarding time average concentration only.

During the preceding decade, two methods were proposed which enable an estimation of the second moment of the concentration field within the framework of a single particle LSPM, with a numerical cost comparable to the one needed for the calculation of the average concentration. The first one is the Volumetric Particle Approach (VPA) [7], which associates a volume to each individual particle (hence the name) and as a result, a so-called “particle concentration”. The second approach, the Virtual Variance Sources (VVS) model [8], stems from the Eulerian equation governing the dynamics of the concentration variance. It takes advantage of the similar dynamics of concentration variance and mean concentration, which differ only by additional source and sink terms which are found in the former.

The two approaches have a few underlying features in common:

- Both involve a calculation of the three-dimensional average concentration field.
- Both require an estimation of a timescale governing the dissipation of concentration fluctuations. This timescale is typically a function of the flow and instantaneous plume width, and therefore changes in space [9].
- The dynamics of the Lagrangian particles which take part in the calculation of the concentration variance is exactly the same as for the particles that are used to calculate the average concentration. This expresses the underlying notion that the fields of concentration variance essentially transport and diffuse through the atmosphere in the same manner other scalars do.

As these two approaches are intended to be used for similar applications, integrated within the same LSPM modeling framework, it is worthwhile to examine them one against the other, in order to detect relative differences in terms of the difficulty of application, unique tendencies, sensitivity to various parameters, and, as far as experimental data is available, success in prediction of concentration variance.

In the current study, the two models are compared by applying them under the same meteorological conditions, the same underlying average concentration field and the same dissipation time scale parameterization. Results of the models are compared to field observations from Intensive Observation Periods (IOPs) 4 and 5 of PSB1 campaign [10], a comprehensive field campaign which included gas releases together with state of the art concentration measurements and meteorological monitoring.

The application of every dispersion model, and specifically the LSPM, involves the estimation of many input meteorological parameters. The importance of determining the amount of error introduced into the model results through the uncertainty in the input parameters is twofold. First, it may help to get a better estimation of the results uncertainty, which is very important for real time risk assessment modeling. Also, relating the uncertainty in each specific input parameter to its effect on the model results can pinpoint key parameters which are to be estimated more accurately, as opposed to others, for which parameter uncertainty does not have dramatic effect over the results. This notion may mark

optimal directions to future work aiming to improve the estimation of key parameters. The dissipation time scale, an essential parameter for both VVS model and VPA is not measured directly and therefore may introduce considerable uncertainty. Here, the sensitivity of the two models to the estimation of dissipation time scale is comparatively investigated by relating the change in the results to controlled changes of the parameter.

Section 2 describes the PSB1 dispersion experiment and meteorological data. Section 3 describes the basic LSPM used for all the models, and the concentration variance models. Section 4 reports the results, first for the average concentration, and then for the concentration variance. The chapter finalizes with a comparative sensitivity analysis. Section 5 concludes the study.

2 Sagebrush phase 1 (PSB1) campaign

The PSB1 campaign [10] carried out by the Field Research Division of the Air Resources Laboratory (ARLFRD) of the National Oceanic Atmospheric Administration (NOAA), was designed to repeat fundamental dispersion experiments in flat terrain, conducted throughout the 1950s and 1960s using state of the art instrumentation unavailable half a century before. Phase 1, which took place in October 2013, in Idaho National Laboratory (INL), focused on continuous releases from a ground source in daytime conditions. Five IOPs were conducted in neutral to unstable conditions. During each IOP, the air downwind from the source was sampled for two hours by integral air samplers arranged in 4 arcs in ranges of 400, 800 1600 and 3200 m from the source. The two hours sampling times consisted of 10 min periods, and the source was triggered half an hour before sampling, to enable steady state formation. Of special importance in the current context is the usage of six high fast response gas analyzers, positioned in different positions, which were sometimes altered during the IOP. The high frequency data measured by these analyzers makes the PSB dataset suitable for the evaluation of concentration fluctuations models.

Meteorological measurements were conducted by sonic anemometers, mounted on a 60 m high mast next to the release location in heights of 2, 4, 8, 16, 30, 45, and 60 m agl (henceforth the GRI tower). Additionally, a sodar systems measured the average wind up to 200 m, and a profiler measured the wind throughout the boundary layer.

During IOPs 1 and 2 the plume occasionally crossed the limits of the sampling field. During IOP3 the plume was steady and stayed inside the sampling field, but much of the high frequency concentration data exceeded the instrument range of detection and therefore was flagged as unreliable. As a result, in this study, only data acquired during IOPs 4 and 5 are used. The meteorological conditions and the resulting average concentration patterns during these IOPs were relatively steady, and the fast response gas analyzers were positioned in constant positions near the main plume axis. For the chosen IOPs the source rate was set to a lower value of 1 g s^{-1} . Consequently, concentrations in the 3200 m sampling arc were too low and were not measured.

3 Models description

In the following section, the Lagrangian framework, used with all the models is shortly described. Also, the VVS model, the VPA and the simple CS model are presented.

3.1 LSPM formulation

The particle equations of motion for the LSPM are [11–13]

$$du_i = -\frac{u_i}{T_i(z)} dt + \frac{1}{2} (1 + u_i^2 / \sigma_i(z)^2) \frac{d\sigma_i(z)^2}{dz} dt + \sigma_i(z) \sqrt{\frac{2dt}{T_i(z)}} \zeta_i \quad (1)$$

$$dx_i = (u_i + U_i(z)) dt \quad (2)$$

where $i = 1, 2, 3$ denote the three dimensional component, u_i is the turbulent velocity of a particle, U_i is the average ambient velocity in the particle location, $\sigma_i(z)$ and $T_i(z)$ are the standard deviation of turbulent velocity and the Lagrangian correlation time, respectively, z is the height a.g.l., dt is the time step and ζ_i is a random variable drawn from a normal distribution with zero mean and unity variance.

The average wind $U_i(z)$ is interpolated from the 10 min averaged sonic anemometer data on the GRI tower, while for elevations higher than the highest anemometer on the tower, average wind is taken from the wind profiler observations. The turbulent standard deviations and Lagrangian time scales are determined by (see [14–16])

$$\begin{aligned} \sigma_u &= \sigma_v = u_* (12 + h/2|L|)^{1/3} \\ \sigma_w &= [1.2w_*^2(1 - 0.9z/h)(z/h)^{2/3} + u_*^2(1.8 - 1.4z/h)]^{0.5} \end{aligned} \quad (3)$$

$$\begin{aligned} T_u &= T_v = 0.15h/\sigma_u \\ T_w &= \begin{cases} \frac{0.1z}{\sigma_w(0.55 - 0.38z/|L|)} & z < |L| \\ 0.59z/\sigma_w & |L| < z < 0.1h \\ 0.15z(1 - e^{-5z/h})/\sigma_w & z > 0.1h \end{cases} \end{aligned} \quad (4)$$

where u_* is the friction velocity, w_* is the convective velocity scale, h is the boundary layer depth, and L is the Monin Obukhov length scale. u_* is estimated by log law curve fit applied for the 3 lowest anemometers on the tower at heights of 2, 4 and 8 m (which is valid whenever $|L| > 8$, which was satisfied throughout IOPs 4 and 5). L and w_* were calculated based on data from the lowest sonic (4 m agl) anemometer on the tower. Good agreement (not shown) is attained when theoretical values for σ_i , Eq. 3, are compared to standard deviations from the sonic anemometers mounted on the tower. The boundary layer depth, h was estimated by radiosonde observations and is 1900 m and 1150 m for IOPs 4 and 5 respectively.

We note that using Eqs. 4–5 as prescribed, the plume width was considerably over predicted. In principle, this implies that either the lateral Lagrangian timescales or the turbulent velocity standard deviations are inadequately prescribed. A choice was made to use the prescribed formulation of the turbulent velocity standard deviation and to reduce the coefficient of the lateral Lagrangian correlation time $T_{u,v}$ by a factor of 0.25, which yielded optimal fit, for the following reasons. First, unlike the timescales, the turbulent velocity standard deviations are directly measured by the sonic anemometers and show agreement with Eq. 3. Secondly, the original derivation of Eq. 4 is indirect and based upon two steps which may introduce uncertainty, namely, relating the peak wavelength of the velocity spectra with the Eulerian timescale and translating from Eulerian to Lagrangian timescales.

100,000 particles were released every 60 s, with average wind and turbulent parameters updated every 10 min. To replicate the experimental procedure, allowing stationarity to be formed prior to the beginning of measurement, release of particles from the source starts half an hour before IOP start time.

3.2 Virtual Variance Sources (VVS) model

The VVS model [10, 11] stems from the steady state Reynolds Averaged equation for the concentration variance, which after adopting K closure approximation, and assuming exponential decay, takes the form

$$-U_i \frac{\overline{\partial c'^2}}{\partial x_i} - \frac{\partial}{\partial x_i} K_i \frac{\overline{\partial c'^2}}{\partial x_i} + 2\sigma_i^2 T_i \left(\frac{\partial \overline{c}}{\partial x_i} \right)^2 - \frac{\overline{c'^2}}{\tau_d} = 0. \quad (5)$$

In this equation τ_d , U_i , K_i , σ_i and T_i are the dissipation time scale, the average wind, the eddy diffusivity, the turbulent velocity components standard deviation and the turbulent correlation time scale and are all a function of space and time. Overbar denotes averaging in the Reynolds Averaged Navier Stokes sense. Equation 5 is similar in form to the simple advection diffusion equation governing the dynamics of a conserved passive scalar, only with a source term (third term), and a decay term (fourth term). As suggested by several authors [18, 19], this implies that the same model used for the average concentration can be used for the concentration variance, with the appropriate definition of a source term and a decay timescale. As the source term contains the gradient of the average concentration, it is mandatory to calculate the average concentration prior to the application of Eq. 4.

Numerically implementing the source term $S \equiv 2\sigma_i^2 T_i \left(\frac{\partial \overline{c}}{\partial x_i} \right)^2$ can be performed by calculating the source term for each grid cell, and consequently, defining a so-called grid *variance mass rate* $Q(\mathbf{r}) = S(\mathbf{r})\Delta V$, where ΔV is the grid cell volume, and \mathbf{r} a location vector associated with the grid cell. The total variance mass of all the particles emitted for the specific grid cell is $\int Q(\mathbf{r})dt$.

For the average concentration fields calculated in this study, 99% of Q is found to be localized within the first 30 m downwind from the origin, and under 10 m in the vertical. Comparing these dimensions to the relevant downwind distances, which are 400 to 1600 m, the source can be regarded as localized. Additionally, as will be explained in the following, the VPA source location and dimensions is equivalent to the real source used for the average concentration. Therefore, to allow proper comparison, it is desirable that the particles will be released from the same location for both models, and experience, statistically, the same decay times along their trajectory. For these reasons, a variance source in the origin is used, emitting ‘variance mass’ of $\int Q(\mathbf{r})dV$ per unit time.

The decay term in Eq. 5 is modeled as an exponential decay of the variance mass carried by each of the particles towards zero. For the far field limit, this tendency naturally results with the appropriate limit of zero variance.

3.3 Volumetric Particle Approach (VPA)

The VPA was independently suggested by [8] and by [20], with each of the authors presenting and justifying the approach differently. For the sake of brevity, we will stick to the

former. The connection between the two presentations of the model has been discussed in [21].

The VPA associates a ‘particle concentration’ c_p and a ‘particle volume’ V_p to every particle. The particle mass is conserved, and thus the particle volume and concentration are related by $m = c_p V_p$, where m is the constant mass per particle. The average concentration in a cell can therefore be expressed as

$$\bar{c} = V_c^{-1} \sum_i^N m_i = \sum_i^N \frac{V_{p_i}}{V_c} c_{p_i}. \quad (6)$$

With V_c the cell volume, and the index i sums over the N particles located in the cell. Following [7], identifying the term $\frac{V_{p_i}}{V_c}$ as a probability distribution function, the second moment can readily be expressed as

$$\overline{c^2} = \sum_i^N \frac{V_{p_i}}{V_c} c_{p_i}^2 = \bar{c} \sum_i^N c_{p_i} = \overline{cc_p}, \quad (7)$$

where the second term from the right stems from a substitution of Eq. 6, and the last term involves the definition of a cell average of particle concentrations $\overline{c_p} = \sum_i^N c_{p_i}$. Consequently, the variance is

$$\overline{c'^2} = \overline{c^2} - \bar{c}^2 = \overline{cc_p} - \bar{c}^2. \quad (8)$$

Following a simplified micromixing approach, c_p interacts with the local average concentration by

$$\frac{dc_p}{dt} = -(c_p - \bar{c})/\tau_d. \quad (9)$$

where τ_d is the dissipation time scale.

For the far field limit $c_p \rightarrow \bar{c}$ and Eq. 9 predicts zero concentration variance, as expected.

It is worth mentioning that the VPA can be naturally used not only for concentration variance modelling of a conserved scalar, but also for the modelling of first and second moments of reacting scalars.

3.4 The dissipation time scale parameterization

As will be further demonstrated in Sect. 4.3, prescribing a correct dissipation time scale has a crucial impact on model performance. Several suggestions have been raised in the literature [7–9, 20] for the parametrization of τ_d . Here, the simple parametrization suggested by [22] will be used, which determines τ_d to be

$$\tau_d = T_s [A_1 r/H + A_2 (d_s/h_s)^{1/3}], \quad (10)$$

with T_s the vertical Lagrangian time scale at the source height, r is the distance from the source, H is the boundary layer height, d_s is the source size, h_s is the source height, and A_1, A_2 are empirical constants to be determined.

To allow comparison under an equal common ground, Eq. 10 was used for both the VVS model and the VPA, where only the constants are modified if necessary.

3.5 Chatwin Sullivan (CS) model

The well-known model by [23], relates the concentration variance to the average concentration by

$$\overline{c'^2} = \beta \bar{c} (\alpha \bar{c}_m - \bar{c}), \quad (11)$$

where \bar{c}_m is the maximal average concentration for the considered downwind distance, and α and β are obtained by best fit to experimental datasets. In a recent wind tunnel study of concentration fluctuations [24], Nironi has reported best fit values of $\alpha = 1.58$ and $\beta = 2.51$, for ground source neutrally stable atmospheric boundary layer.

4 Results

In the following, the model results are presented and compared to the observations, first for the calculated average concentration, and then for the concentration standard deviation.

4.1 Average concentration

The first and necessary stage towards applying the models for concentration fluctuations is the calculation of the three-dimensional average concentration field. We therefore start with comparing predictions for the average concentration with observed average concentration for the two IOPs.

Figure 1 shows the results of the LSPM and the observed concentration for the four 30 min time periods comprising IOP4. Each of the three curves corresponds to a specific sampling arc, where the model results are depicted by solid curves and the observations by connected crosses.

Overall, the calculated average concentration patterns along the arcs are reproduced by the model. We note that even with the diminished lateral Lagrangian time scale used here (see above), the reproduced concentration curves for some of the time periods are sometimes wider than the observed patterns. This is reflected in the scatter plot (Fig. 2), showing that for some cases, the model tends to overestimate the concentration for all ranges. A similar impression is obtained by considering the comparison between modeled and observed values for IOP5 (Appendix A, Figs. 11, 12).

4.2 Concentration variance

Both VPA and VVS were applied using the simple dissipation time scale scheme Eq. 10. However, to obtain optimal agreement with the observations, different constants had to be used. For the VVS the values that were used are $A_1 = 11; A_2 = 0.6875$ and for the VPA higher values (and hence, slower dissipation rates) of $A_1 = 20; A_2 = 1.25$ were prescribed. It is worth noting that in a recent study, Ferrero and Maccarini [17] applied the VVS with substantially higher values of $A_1 = 73.3; A_2 = 1.25$. However, the ranges for that study were of a few hundred meters, whereas here the maximal range is 1600 m.

Figures 3, 4 and 5 present isocontours of the concentration standard deviation, in ppt, for the VPA, VVS and CS models, respectively, during IOP4. In each figure, four subsets

iop4

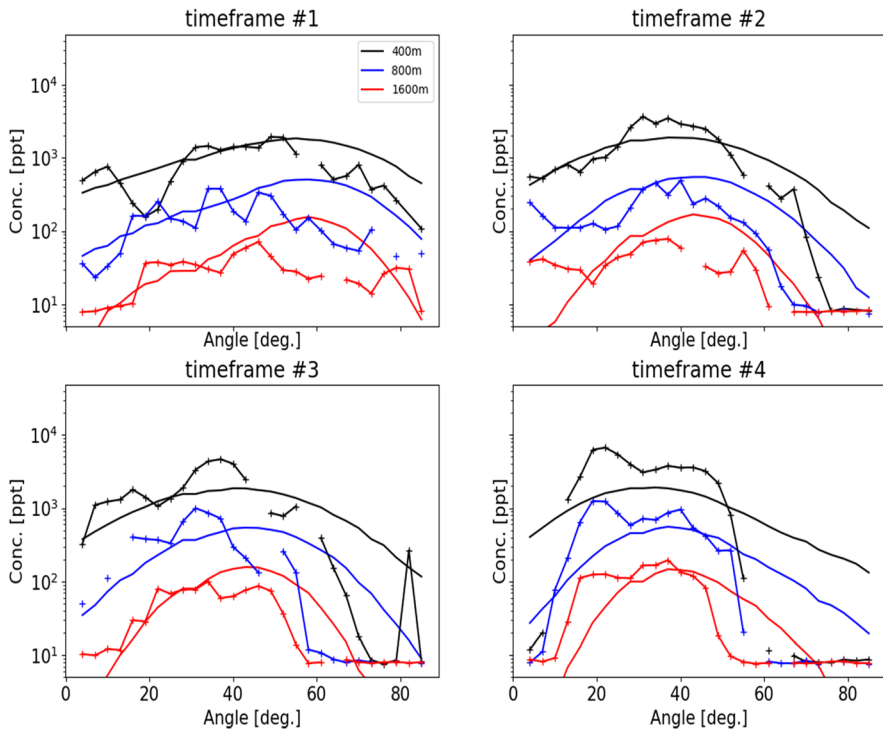


Fig. 1 Predicted (solid curves) and observed (connected crosses) average concentrations for the four 30 Minutes time periods comprising IOP4. Red, blue and black curves correspond to ranges of 400, 800 and 1600 m

correspond to 30 min periods included in the 2 h IOP. The sampling arcs are marked by black crosses in the locations of bag samplers, and red dots correspond to the location of fast response gas analyzers. Text labels near each analyzer location specify the concentration standard deviation measured by this analyzer during the relevant time period.

An evident difference between Figs. 3 and 4 is the status of statistical convergence as qualitatively reflected by the observed contour smoothness. While VPA results exhibit smooth contours, the contours showing VVS results are spotty, with irregular borders, especially in distances of more than 1 km.

To qualitatively evaluate this difference, the ‘touchdown’ statistics for a grid site located on the plume centerline 1500 m downwind from the source and near the ground is examined. During the simulation, every entrance of a particle into the inspection area is accounted for by saving the relevant particle-associated value (c_p for VPM and ‘variance mass’ for the VVS model). The sample normalized standard deviation for increasing sample sizes is plotted in Fig. 6, showing a $1/\sqrt{N}$ convergence for both VVS and VPM, which means that both distributions have a finite second moment, and hence obey the central limit theorem. However, a consistent difference of 2 orders of magnitude between the curves is evident. This implies that to obtain the same level of statistical convergence, the VVS would require 100 times as many particles as the VPM. This considerable difference

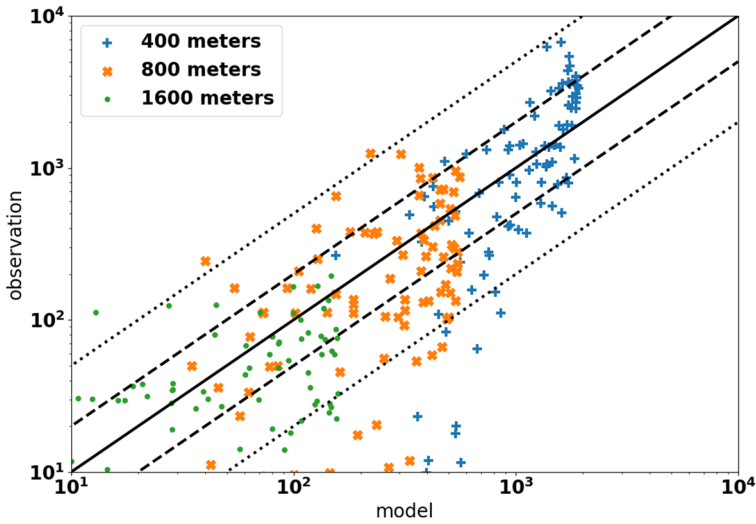


Fig. 2 Scatter plot comparing the predicted (x-axis) and measured (y-axis) average concentrations, in ppt. a solid line presents a perfect match. Dashed and dotted lines depict a factor of 2 and 5, respectively. Different arc ranges are shown in different colors and marker styles

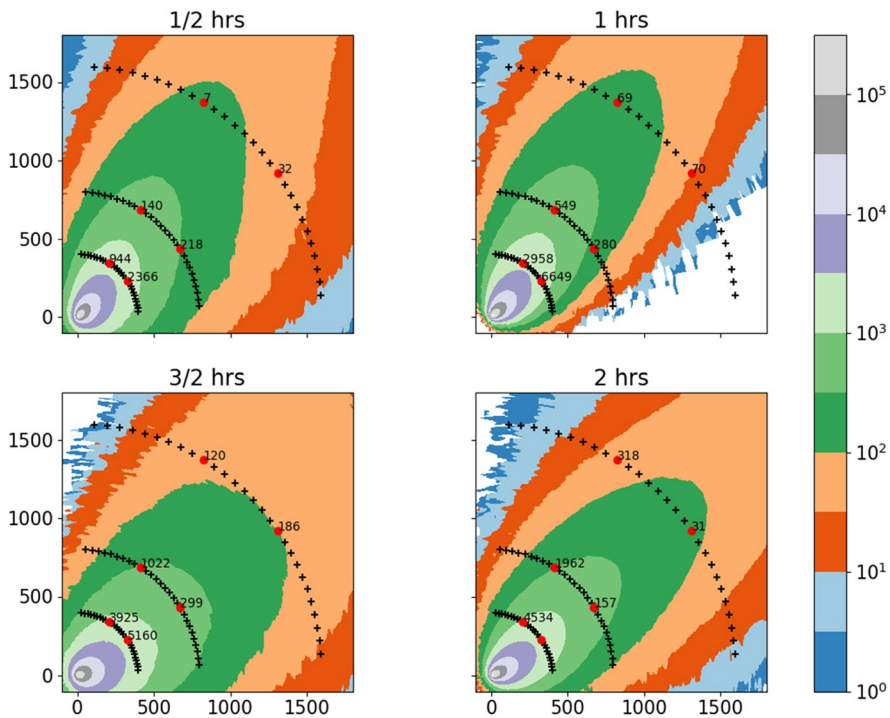


Fig. 3 Isocontours of concentration standard deviation, in ppt, for the VPA model and IOP4. x and y axes show distances in meters, with the release point in the origin. Black crosses mark the positions of bag samplers along the 400, 800 and 1600 m sampling arcs. The four maps correspond to four 30 min time intervals along the IOP. Red dots mark the locations of gas analyzer, with text labels specifying the measured standard deviation

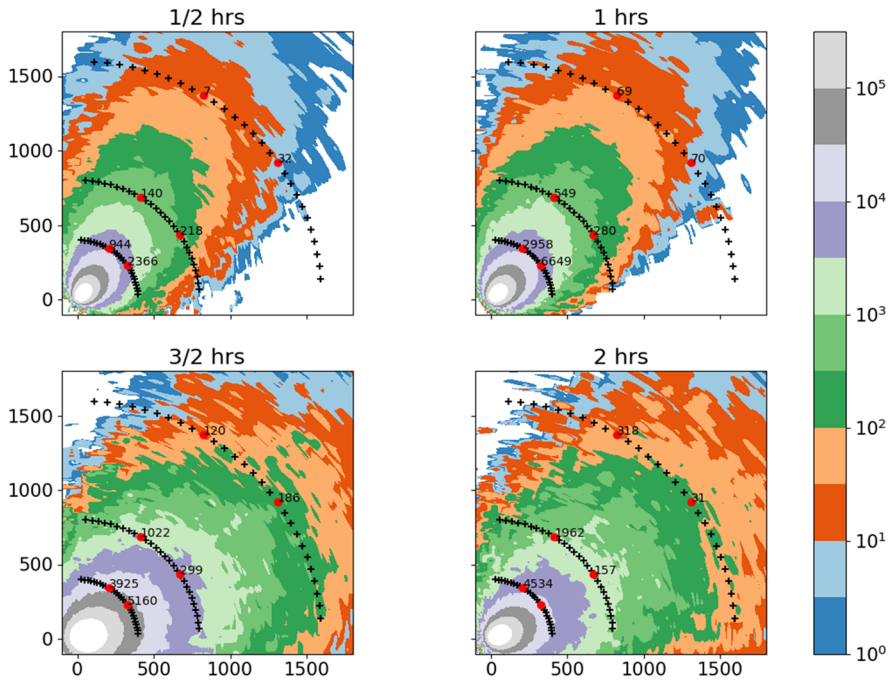


Fig. 4 Like Fig. 3, for the VVS model

is a result of the monotonic exponential decay of each particle's ‘variance mass’ towards zero in the VVS model, which leads to enhanced sensitivity to the history of the particle. In contrast, in the VPA, c_p tends non monotonically towards the local average concentration, which allows a narrower distribution.

Figure 7 presents a scatter plot displaying the amount of agreement between the three models with the observations. The blue, red and purple colors correspond to VPA, VVS and CS, and the range (400, 800 and 1600) is reflected by the marker type. A solid curve shows the ideal match and dashed and dotted curves mark factor 2 and factor 5 differences. All models suffer from increased discrepancies in the far field. While most of the VPA results reside within a factor of 2 or 3 from the observations, VVS results show a somewhat lower agreement with observations, with a tendency of overestimation in the near field. The simple CS model exhibits overall comparable performance to the two more sophisticated models, specifically for shorter ranges (higher standard deviation values).

A similar scatter plot for IOP5 is presented in Fig. 8 (contour plots for IOP5 are presented in Appendix B). While VPA and CS retain similar performance to IOP4, VVS show underestimation in the far field, which was not observed for IOP4.

4.3 Sensitivity to dissipation time

For the VPA and VVS models, a unique input parameter which is not estimated for average concentration dispersion models is the dissipation time length. The estimation of the parameter is complex as it depends on the plume topology as well as on the atmospheric flow and turbulence. For that reason, it is reasonable to assume that the parametrization

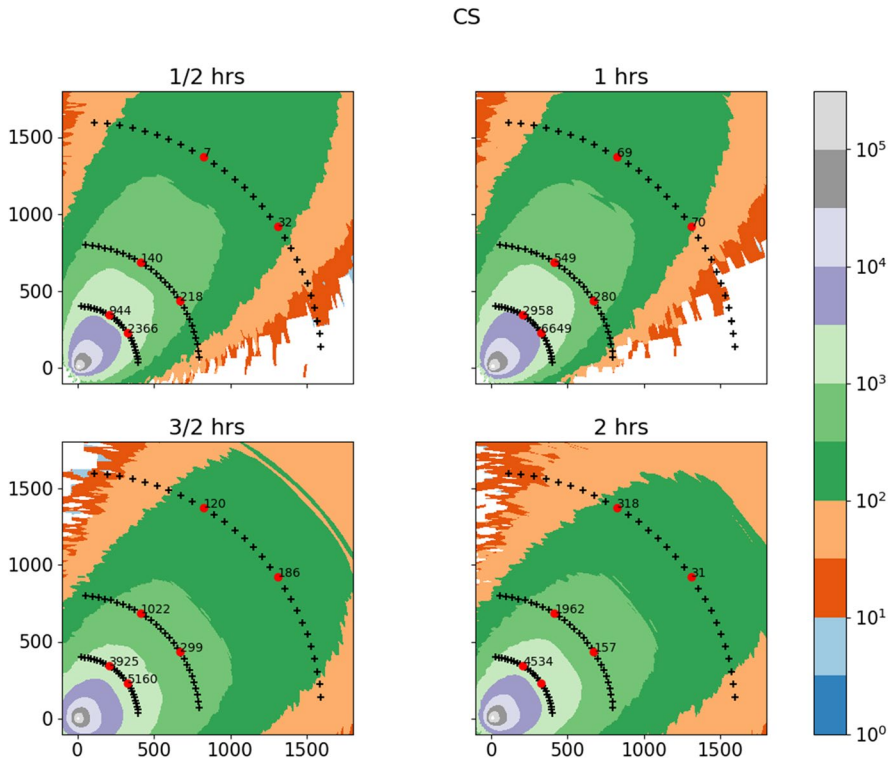


Fig. 5 Like Fig. 3, for the CS model

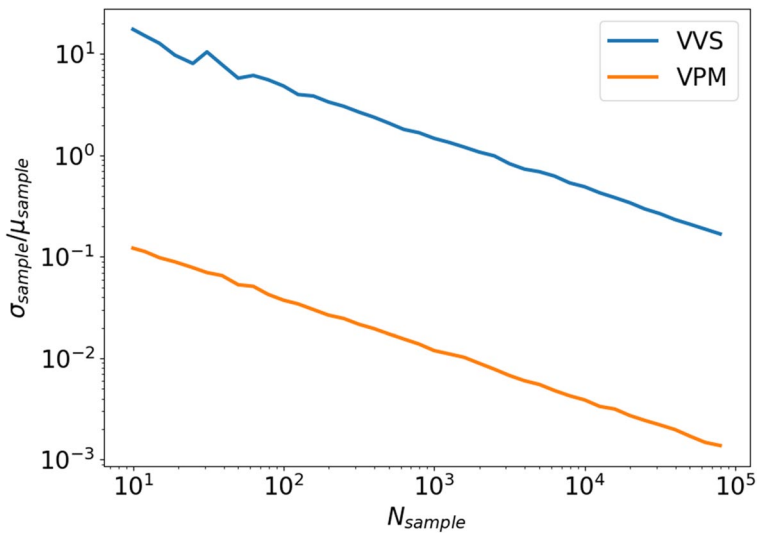


Fig. 6 Sample standard deviation normalized by the sample mean, for samples of increasing size drawn from particle 'touchdown' values of a specific area 1500 m downwind on the plume axis. The blue curve corresponds to the VVS model, and an orange curve corresponds to the VPA

Fig. 7 Predictions of the three models (x-axis) and observations (y-axis) in ppt, for IOP4, presented in a scatter plot. The blue, red and purple colors correspond to VPA, VVS and CS, and the range (400, 800 and 1600) is reflected by the marker type. Solid, dashed and dotted curves mark an ideal match, factor 2 and factor 5 differences, respectively

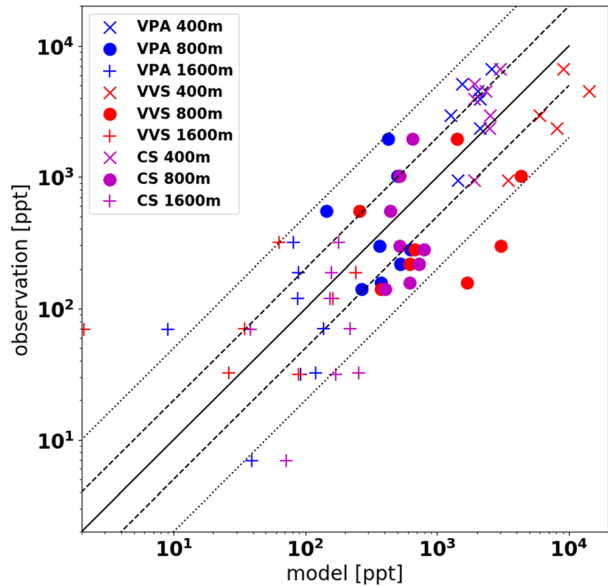
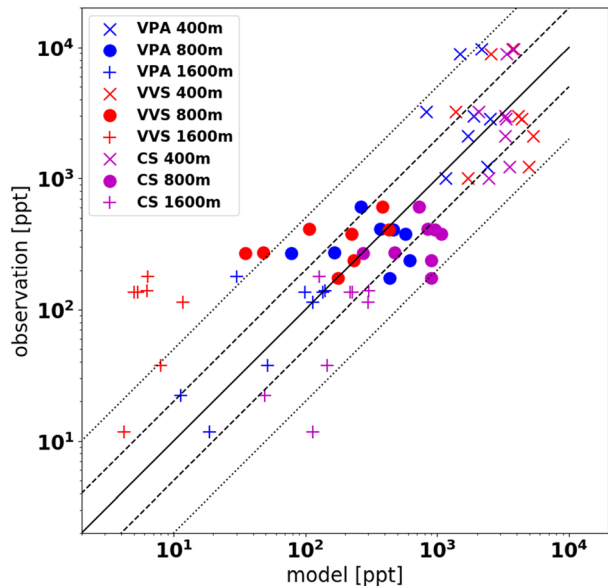


Fig. 8 Like Fig. 7 for IOP5



of the dissipation time involves considerable uncertainty which may play an important role in quantifying the uncertainty of the models prediction for real life applications.

The VPA and VVS model were run with a slight change of the dissipation time. The dissipation time scale was increased and decreased by 20%. Naturally, a decrease of the

Fig. 9 A scatter plot comparing VVS model predictions and observations of concentration standard deviation in ppt, for an increased (red crosses) and a decreased (blue crosses) dissipation time scale

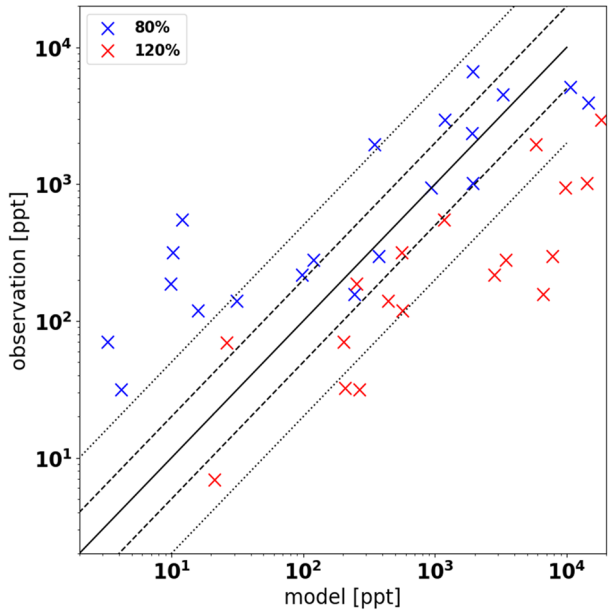
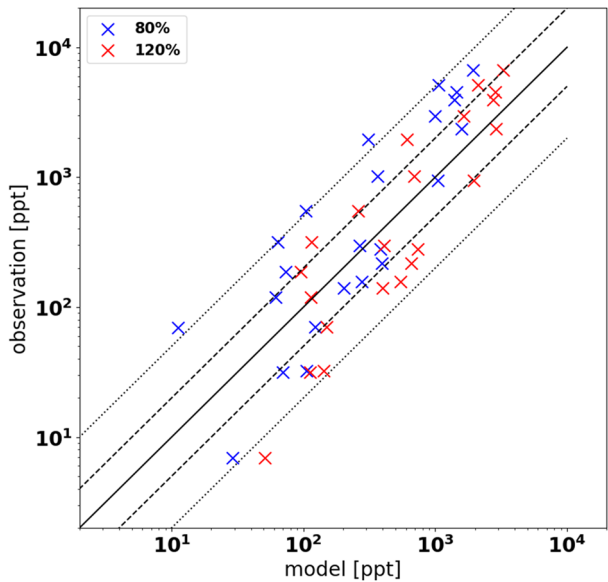


Fig. 10 Like Fig. 9 for the VPA model



time scale leads to lower values of concentration standard deviation, and vice versa for an increase of the time scale.

Figure 9 shows the VVS model predictions against the observations when the dissipation time scale increases (red crosses) and decreases (blue crosses). A considerable

difference, up to an order of magnitude, is observed. When the same procedure is applied for the VPA (Fig. 10), smaller differences of two to three-fold are evident.

5 Discussion and conclusion

Unlike the modeling of average concentration, which is well established, based upon tens of years of research, the study of concentration fluctuations modeling has gained much less attention. Likewise, contrary to the abundance of experimental data acquired in multiple field experiments of averaged concentration, measurements of concentration fluctuations demand high frequency analyzers and are therefore much more complex and rare. Consequently, a serious gap remains between the theoretical knowledge of concentration fluctuations modeling, and its utilization for real life hazard assessment applications.

This work aims to bring the most recent practical approaches for concentration fluctuation modeling closer to real life implementations by comparing two promising approaches, the VVS model and the VPA, by evaluating them against experimental data, and comparing them to each other. Also, the simple CS model was also included in the study, to evaluate the relative consequences of implementing a more basic model, which can be easily implemented on the top of an existing T&D model, for simple flat topography scenarios.

To isolate relevant factors, the comparison was made on a ground as common as possible. The same source topology and implementation, average concentration field, meteorology and particle dynamics and dissipation time scale parameterization were used for each of the models.

Consistent with former work, both models were found to predict concentration fluctuations satisfactorily. Also, the CS model performed comparably to the more sophisticated models.

An aspect which has practical significance is the statistical convergence, which determines the number of Lagrangian particles that has to be used. Differences in the modeling of the concentration fluctuations decay between the VVS model and the VPA results in a wider distribution of the values carried by the particle for the former. Thus, more particles are needed to attain sufficient statistical convergence for the VVS model.

Another aspect of practical importance is the sensitivity of the models predictions to uncertainty in the estimation of the dissipation time scale. This parameter is essential for the modeling, and is never measured directly, which reasonably results in a considerable level of uncertainty. It was found that the VPA is more robust to changes in the dissipation time scale. In this respect, it may be more suitable for practical applications for which uncertainty more likely exists.

Appendix A: average concentrations IOP5

This appendix presents average concentration results for IOP5. See Figs. 11 and 12.

iop5

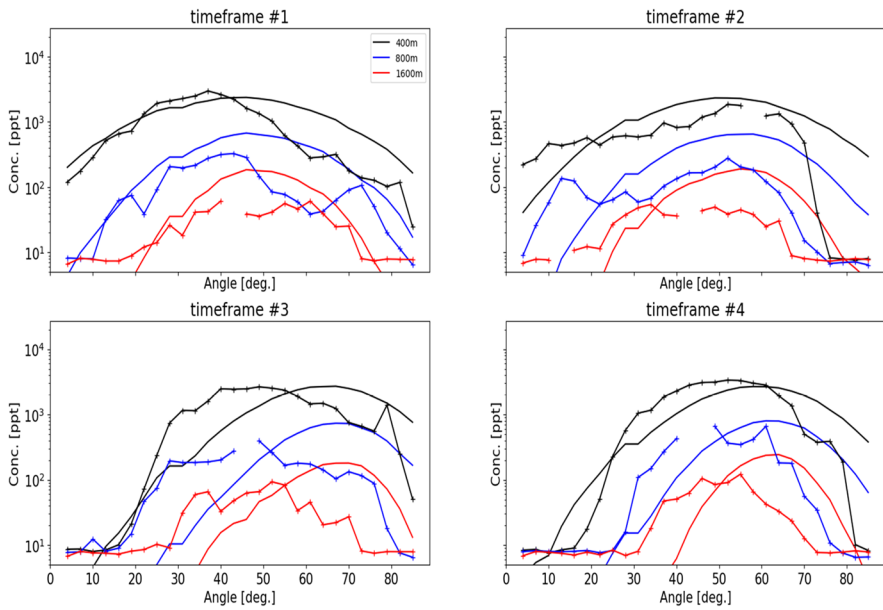


Fig. 11 Like Fig. 1, for IOP5

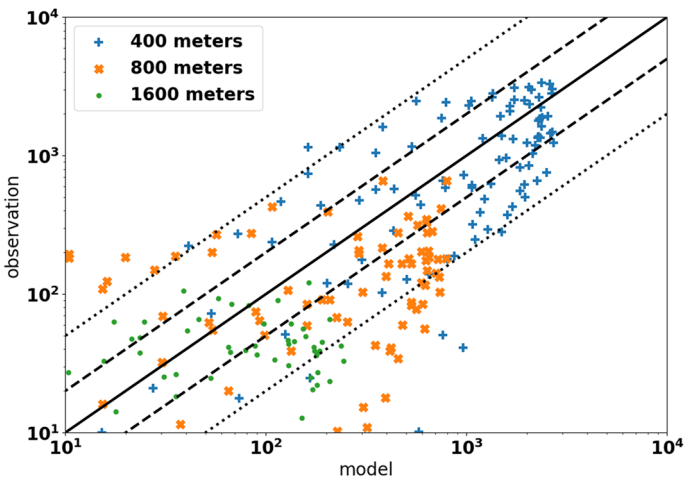


Fig. 12 Like Fig. 2. For IOP5

Appendix B: standard deviation contours IOP5

This appendix presents second moment results for IOP5. See Figs. 13, 14 and 15.

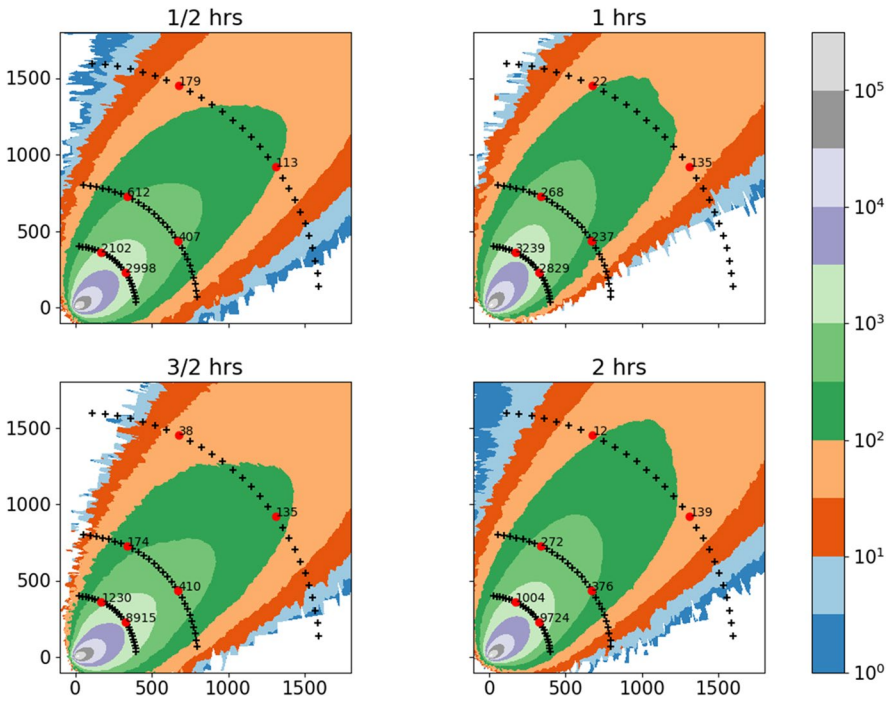


Fig. 13 Like Fig. 3. For IOP5

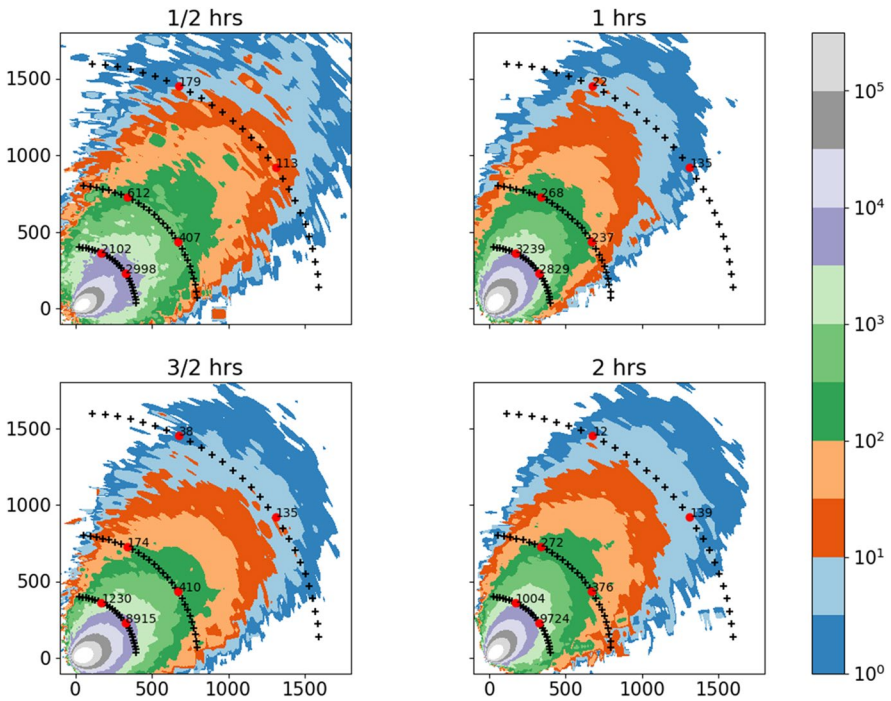


Fig. 14 Like Fig. 4. For IOP5

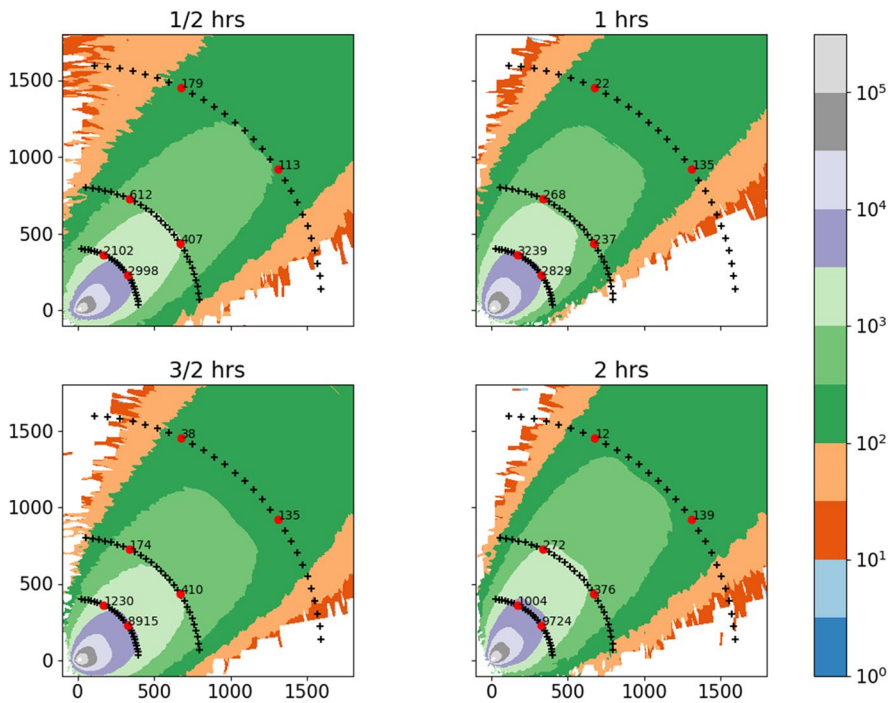


Fig. 15 Like Fig. 5. For IOP5

Acknowledgements We thank the Field Research Division of the Air Resources Laboratory (ARLFRD) of the National Oceanic Atmospheric Administration (NOAA) for the PSB1 data. We thank the IMOD for the funding of this research.

Author contributions AM is the sole contributor of this work.

Funding This work was supported by the Israeli Ministry of Defense.

Declarations

Competing interest The authors declare that they have no known competing financial interests or personal relationships that could have appeared to influence the work reported in this paper.

References

1. Wilson DJ (2010) Concentration fluctuations and averaging time in vapor clouds. Wiley
2. Cassiani M, Bertagni MB, Marro M, Salizzoni P (2020) Concentration fluctuations from localized atmospheric releases. *Bound-Layer Meteorol* 177(2):461–510
3. Hilderman TL, Hrudehy SE, Wilson DJ (1999) A model for effective toxic load from fluctuating gas concentrations. *J Hazard Mater* 64(2):115–134
4. Ferrero E, Oetli D (2019) An evaluation of a Lagrangian stochastic model for the assessment of odours. *Atmos Environ* 206:237–246
5. Manor A, Marx S, Aharoni R (2019) High-fidelity simulations of Chemical Plume Tracing in the planetary boundary layer. *Atmos Environ* 198:313–323
6. Taylor GI (1922) Diffusion by continuous movements. *Proc Lond Math Soc* 2(1):196–212

7. Cassiani M (2013) The volumetric particle approach for concentration fluctuations and chemical reactions in Lagrangian particle and particle-grid models. *Bound-Layer Meteorol* 146(2):207–233
8. Manor A (2014) A stochastic single-particle Lagrangian model for the concentration fluctuations in a plume dispersing inside an urban canopy. *Bound-Layer Meteorol* 150(2):327–340
9. Sykes RI, Lewellen WS, Parker SF (1984) A turbulent-transport model for concentration fluctuations and fluxes. *J Fluid Mech* 139:193–218
10. Finn D, Clawson KL, Eckman RM, Carter RG, Rich JD, Strong TW, Beard SA, Reese BR, Davis D, Liu H, Russell E, Gao Z, Brooks S (2015) Project Sagebrush Phase 1. NOAA technical memorandum OAR ARL-268. Air Resources Laboratory, Idaho Falls, Idaho, p 338. <https://doi.org/10.7289/V5VX0DHV>
11. Thomson DJ (1984) Random walk modelling of diffusion in inhomogeneous turbulence. *Q J R Meteorol Soc* 110:1107–1120
12. Thomson DJ (1987) Criteria for the selection of stochastic models of particle trajectories in turbulent flows. *J Fluid Mech* 180:529–556
13. Wilson JD, Legg BJ, Thomson DJ (1983) Calculation of particle trajectories in the presence of a gradient in turbulent-velocity variance. *Boundary-layer Meteorol* 27:163–169
14. Hibberd MF, Sawford BL (1994) A saline laboratory model of the planetary convective boundary layer. *Bound-Layer Meteorol* 67(3):229–250
15. Brost RA, Wyngaard JC, Lenschow DH (1982) Marine stratocumulus layers. Part II: turbulence budgets. *J Atmos Sci* 39(4):818–836
16. Hanna SR (1984) Applications in air pollution modeling. In: Nieuwstadt FTM, Dop H (eds) *Atmospheric turbulence and air pollution modelling*. Springer, Dordrecht, pp 275–310
17. Ferrero E, Maccarini F (2021) Concentration fluctuations of single particle stochastic Lagrangian model assessment with experimental field data. *Atmosphere* 12(5):589
18. Netteville DDJ (1979) Concentration fluctuations in plumes. Syncrude Canada Ltd., Edmonton, Alberta. *Environmental Research Monograph* 1979-4. pp 228
19. Wilson DJ, Fackrell JE, Robins AG (1982) Concentration fluctuations in an elevated plume: a diffusion–dissipation approximation. *Atmos Environ* 1967 16(11):2581–2589
20. Kaplan H (2014) An estimation of a passive scalar variances using a one-particle Lagrangian transport and diffusion model. *Physica A* 393:1–9
21. Ferrero E, Manor A, Mortarini L, Oetl D (2020) Concentration fluctuations and odor dispersion in Lagrangian models. *Atmosphere* 11(1):27
22. Ferrero E, Mortarini L, Purgè F (2017) A simple parametrization for the concentration variance dissipation in a Lagrangian single-particle model. *Bound-Layer Meteorol* 163(1):91–101
23. Chatwin PC, Sullivan PJ (1993) The structure and magnitude of concentration fluctuations. *Bound-Layer Meteorol* 62(1):269–280
24. Nironi C (2013) Concentration fluctuations of a passive scalar in a turbulent boundary layer. Dissertation, Ecole Centrale de Lyon

Publisher's Note Springer Nature remains neutral with regard to jurisdictional claims in published maps and institutional affiliations.

Springer Nature or its licensor (e.g. a society or other partner) holds exclusive rights to this article under a publishing agreement with the author(s) or other rightsholder(s); author self-archiving of the accepted manuscript version of this article is solely governed by the terms of such publishing agreement and applicable law.